DEMIXING MULTIVARIATE-OPERATOR SELF-SIMILAR PROCESSES

Gustavo Didier[(1)], *Hannes Helgason*[(2)], *Patrice Abry*[(3)]

[(1)] Mathematics Dept., Tulane University, New Orleans-LA, USA, gdidier@tulane.edu
[(2)] School of Engineering and Natural Sciences, University of Iceland, hannes.helgason@gmail.com,
[(3)] Physics Dept., Ecole Normale Supérieure de Lyon, CNRS, France, patrice.abry@ens-lyon.fr
Supported by ANR BLANC 2011 AMATIS BS0101102, Louisiana Board of Regents award LEQSF(2008-11)-RD-A-23
GD and HH's long term visiting positions at ENS-Lyon were supported, respectively, by ENS-Lyon and the
French Academy of Sciences Young Research Team award

ABSTRACT

Operator self-similarity naturally extends the concepts of univariate self-similarity and scale invariance to multivariate data. Beyond a vector of Hurst parameters, operator self-similarity models also involve a mixing matrix. The present contribution aims at estimating the collection of Hurst parameters in the case where the mixing matrix is not diagonal. To the best of our knowledge, this has never been achieved. In addition, the mixing matrix is also identified. The devised procedure relies on a source separation methodology, since the underlying components of the operator self-similar process are assumed to have a diagonal pre-mixing covariance structure. The principle behind the demixing procedure is illustrated based on synthetic 4-variate operator self-similar processes, with a priori prescribed and controlled Hurst parameters and mixing matrix. Identification and estimation performance for both Hurst parameters and mixing matrices are shown to be very satisfactory, using large size Monte Carlo simulations.

Index Terms— multivariate scale invariance, operator self-similarity, source separation, mixing, identification.

1. INTRODUCTION

Scale invariance and self-similarity. The paradigm of scale invariance is commonly used to analyze signals or systems where no particular time scale can be singled out as playing a special role in driving temporal dynamics. Instead, scale invariance implies that a large continuum of time scales are all contributing to temporal dynamics. When analyzing such signals, the focus is hence no longer on identifying specific scales of time, but rather on evidencing mechanisms that relate all scales together, often quantified by scaling exponents (cf. e.g., [1, 2, 3, 4, 5]).

Stationary increment self-similar processes such as the (Gaussian) fractional Brownian motion (fBm) [6] have been widely used as touchstone models for scale invariance. Self-similarity means that the signal X cannot be (statistically) distinguished from any of its dilated versions: $\{X(t)\}_{t\in\mathbb{R}} \stackrel{f.d.d.}{=} \{a^H X(t/a)\}_{t\in\mathbb{R}}$, $a > 0$, where H is referred to as the self-similarity, or Hurst, parameter, and $\stackrel{f.d.d.}{=}$ refers to equality of finite dimensional distributions. Self-similarity also implies that the moments of order $q > -1$ of the wavelet coefficients $d_X(j,k)$ of X behave as power laws with respect to the analysis scale $a = 2^j$ [4, 7, 8] $(j, k \in \mathbb{Z},\ \ j \geq 0\ )$:

$$\mathbb{E}|d_X(j,k)|^q = \mathbb{E}|d_X(0,0)|^q 2^{jq(H+1/2)}. \qquad (1)$$

With such models, the practical analysis of scale invariance fundamentally amounts to determining the range of scales where the power law behavior holds and to estimating the parameter H (cf. e.g., [5] and references therein for a review). Most estimation procedures for H rely on exploiting the power law behavior in Eq. 1 (cf. e.g., [9] for a review). Self-similarity has been used as a powerful model to analyze numerous signals and systems from a wide-ranging spectrum of applications comprising natural systems (hydrodynamics turbulence [10], geophysics [11], heart rate variability [12], infraslow (i.e., below 1Hz) brain activity [13, 14], genomics [15]) or man-made systems (Internet traffic [16, 5], finance [17], population growth [18], to list but a few).

Multivariate self-similarity. In the modern era, with technological developments and mass production, it is common that one same system is monitored with a large number of sensors, thus naturally leading to a collection of P signals recorded jointly, i.e., multivariate data $\mathbb{R} \to \mathbb{R}^P$. Yet, in most applications, scale invariance analysis has remained univariate: each signal is analyzed independently. A generalization of fBm, Operator-fBm (OfBm) has recently been proposed as a multivariate Gaussian self-similar model [19, 20, 21, 22]. OfBm can be essentially defined by the linear mixing, via a $P \times P$ matrix W, of P fBms, each with a (potentially) different self-similarity parameter, thus defining a vector of parameters $\underline{H} = \{H_1, \ldots, H_P\}$, and made correlated by a $P \times P$ point covariance matrix Σ.

Related Work: OfBm identification. Though conceptually appealing as a model to account for multivariate scale invariance in data, OfBm has seldom been used in applications, mostly because it is far more complicated than its counterpart fBm. Indeed, modeling based on OfBm requires the estimation not only of a single scaling parameter H, or even of P scaling parameters $\underline{H}$, but also of two additional $P \times P$ matrices W and Σ. The latter may convey information on the (physical, physiological,...) mechanisms underlying data production which is as crucial as that provided by the scaling exponents themselves. The particular case where no mixing is present, i.e., W is diagonal, has already been theoretically well-analyzed in several contributions [21, 23]. In [24], wavelet based tests were devised aiming at assessing whether or not the cross-dependencies of multivariate data followed OfBm models. In applications, OfBm models with diagonal W have notably been used to analyze infraslow brain activity: beyond the traditional estimation of scaling parameters $\underline{H}$ (cf. e.g., [25]), it has been recently and successfully used to assess task performance prediction [14]. Furthermore, functional connectivity (i.e., the way various regions of the brain interact) is traditionally assessed by measuring correlations amongst signals associated to each region of the brain [26]. Yet, OfBm models show that correlation amongst components results from the interplay between W and Σ. It is thus natural to wonder whether functional connectivity should be assessed based on the overall correlation between components (i.e., mixing the contributions of both W and Σ) or, rather, on unmixed components Σ. To address this type of question, it is crucial to estimate W in situations where W is not diagonal. However, to the best of our knowledge, the full identification of OfBm, i.e., the estimation of its $\frac{3}{2}(P + P^2)$ parameters $\underline{H}, W, \Sigma$, has never been addressed, despite its paramount importance in applications.

Goals, contributions and outline. The present contribution is a first step toward the general and ambitious goal of fully identifying OfBm. The focus here is on the particular case where the underlying covariance matrix Σ is diagonal but W is *not*: the observed components are correlated due to mixing, whereas the underlying fBm components are uncorrelated. This models the very interesting situation where the signals from various originally independent subparts of a system get mixed up by a number of sensors recording them. The present contribution devises a joint estimation procedure for the mixing matrix W and the vector of Hurst parameters $\underline{H}$. It relies on the combination of source separation techniques (joint diagonalization algorithms) and wavelet decompositions (described in Sections 2.2 and 2.3, respectively) applied to the specific subclass of OfBms with diagonal Σ (cf. Section 2.1). The principle behind the demixing procedure is illustrated using P-variate synthetic OfBms with prescribed W and $\underline{H}$. The estimation performance is assessed via large size Monte-Carlo simulations (cf. Section 3).

2. THEORY AND METHODOLOGY

2.1. Operator-fBm with diagonal Σ

Operator self-similarity. The general definition of OfBm can be found in [19, 21]. Here, definitions are restricted to the case of diagonal Σ. For $0 < H_1 \leq H_2 \leq \ldots \leq H_p < 1$, let $\underline{B}_{\underline{H}}(t) \equiv \{B_{H_p}(t), t \in \mathbb{R}, p = 1, \ldots, P\}$ denote P-independent fBms with covariance functions

$$\mathbb{E}B_{H_p}(t)B_{H_p}(s) = \sigma_p^2/2(|t|^{2H_p} + |s|^{2H_p} - |t-s|^{2H_p}). \quad (2)$$

Let W denote a $P \times P$ invertible matrix. The subclass of OfBm $\underline{B}_{\underline{H}}^W$ of interest here is defined as $\underline{B}_{\underline{H}}^W \equiv W\underline{B}_{\underline{H}}$. It corresponds to the subset of the largest class of OfBm obtained by imposing $\Sigma \equiv Id$ and diagonalizable matrix $H_W \equiv W^T diag(\underline{H})W$ [19]. The stationary increment processes $\underline{B}_{\underline{H}}^W$ are operator self-similar, i.e., $\{\underline{B}_{\underline{H}}^W(at)\}_{t\in\mathbb{R}} \overset{fdd}{=} \{a^{H_W}\underline{B}_{\underline{H}}^W(t)\}_{t\in\mathbb{R}}, \forall a > 0$, with $a^{H_W} = \sum_{k=0}^{\infty} \log^k(a)H_W^k/k!$. By contrast, the entrywise processes making up $\underline{B}_{\underline{H}}$ are univariate self-similar, i.e., $\forall p = 1, \ldots, P$, $\{B_{H_p}(at)\}_{t\in\mathbb{R}} \overset{fdd}{=} \{a^{H_p}B_{H_p}(t)\}_{t\in\mathbb{R}}$, $a > 0$. Assuming a priori that Σ is diagonal, the goal of the present contribution is to jointly estimate the vector of Hurst parameters $\underline{H}$ and the mixing matrix W, from the sole observation of the *mixed* data $\underline{B}_{\underline{H}}^W$.

Covariances. Let $X_p(k) = B_{H_p}(k+1) - B_{H_p}(k)$ and $Y_p(k) = B_{H_p}^W(k+1) - B_{H_p}^W(k)$ denote the increments of the original process B_{H_p} and its mixed counterpart $B_{H_p}^W$. Let $\Sigma_X(\tau) = \mathbb{E}X_p(k)X_{p'}(k+\tau)$ denote the covariance of X: $\Sigma_X(\tau) \equiv diag(\sigma_1^2 r_{H_1}(\tau), \ldots, \sigma_P^2 r_{H_P}(\tau))$, with:

$$r_{H_p}(\tau) \equiv |\tau+1|^{2H_p} + |\tau-1|^{2H_p} - 2|\tau|^{2H_p}. \quad (3)$$

By definition, $\underline{Y} \equiv W\underline{X}$. Thus, the covariance of $\underline{Y}$ involves both parameters W and $\underline{H}$: $\Sigma_Y(\tau) = W\Sigma_X(\tau)W^T$.

Ambiguity factors or under-determination. In practice, we only observe $\underline{Y}$ and try to estimate both W and $\underline{H}$, thus $\Sigma_X(\tau)$. Starting from the covariance $\Sigma_Y(\tau)$, there are three forms of ambiguities, or under-determination, in the identifiability of W: First, for $\tau = 0$:

$$\begin{aligned}\Sigma_Y(0) &= \mathbb{E}\underline{Y}\underline{Y}^T = W\underline{X}\underline{X}^T W^T = W\Sigma W^T \\ &= W diag(\sigma_1^2, \ldots, \sigma_P^2)W^T = W' Id W'^T,\end{aligned}$$

with $W' = W diag(\sigma_1, \ldots, \sigma_P)$. Thus, $\underline{Y} = W\underline{X} = W'\underline{X'}$, with $\Sigma_{X'}(0) \equiv \Sigma = Id$. Second, let Π denote a $P \times P$ permutation matrix, i.e., with only one non-zero entry (equal to 1) per column and lines, then, $\underline{Y} = W\underline{X} = W'\underline{X'}$ with $W' = W\Pi$ and $X' = \Pi^T X$. Third, each column of W can be individually multiplied by ± 1, leading to $W' = WS$. Here, S is a diagonal matrix with entries ± 1, and $X' = S^T X$, such that $\underline{Y} = W\underline{X} = W'\underline{X'}$, with $\Sigma_{X'}(0) \equiv \Sigma = Id$.

2.2. Source separation based demixing procedure

Identifiability. Starting from one single observation of finite length n of a P-variate process $\underline{Y}$, the goal is to devise a *demixing* procedure yielding an estimate $\widehat{W^{-1}}$ of W^{-1} such that process $\underline{Z} = \widehat{W^{-1}}\underline{Y}$ has a covariance matrix $\Sigma_Z(\tau)$ as close as possible to the covariance $\Sigma_X(\tau)$ of $\underline{X}$. In other words, $\Sigma_Z(\tau)$ should be diagonal for all τ. Following the terminology commonly used in blind source separation (cf. e.g., [27]), it will be said that an invertible matrix W is *identifiable* when it can be estimated from a single observation Y, up to the ambiguity factors listed in Section 2.1.

Theorem. An invertible matrix W is identifiable if and only if all parameters H_p are different: $\forall(p,p') \in [1,\dots,P]^2, 0 < H_p \neq H_{p'} < 1$.

The proof is straightforward, as blind source separation theory teaches us that the identifiability of Gaussian processes requires the pairwise linear independence of the processes X_p. In addition to $\mathbb{E}X_p(t)X_{p'}(t+\tau) \equiv 0$, the latter condition implies that the covariance functions of X_p and $X_{p'}$ cannot be proportional.

Joint Diagonalization. Let $\{\hat{\Sigma}_Y(\tau_m), m = 0,\dots,M\}$, $M > 1$, denote the sample covariance matrices of $\underline{Y}$ at lags τ_m. Given that the target process $\underline{Z} = \widehat{W^{-1}}\underline{Y}$ should have diagonal covariance matrices for all τ, we can rely on some strategy from blind source separation (cf. e.g., [27]) to develop a *demixing* matrix $\widehat{W^{-1}}$ that achieves the joint diagonalization of $\hat{\Sigma}_Y(\tau_m)$, $\forall\tau_m$. In the present contribution, we will focus on the particular choice $M = 2$, i.e., $\Sigma_Y(\tau)$ is estimated for two different lags $\tau_1 \equiv 0$ and $\tau_2 \equiv \tau$. This enables us to perform an exact joint diagonalization of $\hat{\Sigma}_Y(0)$ and $\hat{\Sigma}_Y(\tau)$ by means of the following procedure [28]:

Step0: From one observation $\underline{Y}$, estimate $\hat{\Sigma}_Y(0)$, $\hat{\Sigma}_Y(\tau)$;

Step1: Set $\Theta = \hat{\Sigma}_Y(0)^{-1/2}$;

Step2: Find eigenvectors Q of the matrix $\Theta\hat{\Sigma}_Y(\tau)\Theta^T$;

Step3: Define $\widehat{W^{-1}} = Q\Theta$.

To prove that this method permits the identification of W, assume that $\Sigma_Y(0)$ and $\Sigma_Y(\tau)$ are known, and used instead of their estimates. Also, assume that $\Sigma \equiv Id$. Let $W = VO$ denote the polar decomposition of W, i.e., V is positive definite and O is an orthogonal matrix. Given that $\Sigma_Y(0) = W^T\Sigma_X(0)W = W^T\Sigma W = W^TW$, we have that $\Sigma_Y(0) = VOO^TV^T = VV^T$. Thus, in Step 1, $\Theta = V^{-1}$. By definition, $\Sigma_Y(\tau) = W^T\Sigma_X(\tau)W$, with $\Sigma_X(\tau)$ diagonal. Therefore, $\Theta\Sigma_Y(\tau)\Theta^T = V^{-1}VO\Sigma_X(\tau)O^TV^TV^{-1^T} = O\Sigma_X(\tau)O^T$, which thus leads to $Q \equiv O^T$. Thus, Step 3 yields $\widehat{W^{-1}} = O^TV^{-1} = W^{-1}$, as desired.

Under-determination. To address the three ambiguity factors listed in Section 2.1, the following rules are applied to the output $\widehat{W^{-1}}$ of Step 3: First, each column of $\widehat{W^{-1}}$ is multiplied by a positive number such that squared entries of the column sum to 1. Second, columns of $\widehat{W^{-1}}$ are permuted so that the estimated $\hat{H}_p$ for each component of $\underline{Z} = \widehat{W^{-1}}\underline{Y}$ (using the procedure detailed in Section 2.3) are sorted by increasing order. Third, each column p of the permuted matrix $\widehat{W^{-1}}$ is multiplied by the sign of the entry $\widehat{W^{-1}}(p,p)$.

2.3. Wavelet based Hurst parameter estimation

Wavelet coefficients. The estimation of the Hurst parameters is conducted under the classical wavelet framework devised in [4]. Let ψ be a mother wavelet, characterized by its uniform regularity index and number of vanishing moments N_ψ. The latter is a positive integer, defined as $\forall n = 0,\dots,N_\psi-1$, $\int_{\mathbb{R}} t^k\psi(t)dt \equiv 0$ and $\int_{\mathbb{R}} t^{N_\psi}\psi(t)dt \neq 0$. Let $\{\psi_{j,k}(t) = 2^{-j/2}\psi(2^{-j/2}t-k)\}_{(j,k)\in\mathbb{N}^2}$ denote the collection of dilated and translated templates of ψ that form an orthonormal basis of $\mathcal{L}^2(\mathbb{R})$. The discrete wavelet transform coefficients of a univariate signal f are defined as $d_f(j,k) = \langle\psi_{j,k}|f\rangle$. For a detailed introduction to wavelet transforms, see [29].

Estimation of H. For entrywise self-similar processes f with scalar Hurst parameter H, it is well-known that $\mathbb{E}|d_f(j,k)|^2 = 2^{j(2H+1)}$. Following [4], the estimation of the parameter H is carried out by means of a weighted linear regression in a $\log_2 S_f(j)$ versus $\log_2 2^j = j$ diagram, with

$$S_f(j) = \left(\sum_{k=1}^{n_j} |d_f(j,k)|^2\right)/n_j, \tag{4}$$

over a range of scales $j_1 \leq j \leq j_2$. The w_j represent the usual weighted linear regression coefficients (cf. e.g., [4]) leading to the estimator

$$\hat{H} = \frac{1}{2}\Big(\sum_{j=j_1}^{j_2}(w_j \log_2 S_f(j)) - 1\Big). \tag{5}$$

3. DEMIXING PRINCIPLE AND PERFORMANCE

To illustrate the principle behind the proposed demixing procedure and to assess its statistical performance, we have set up the following pedagogical protocol. We synthesize $R = 1,000$ realizations of OfBms with $P = 4$, size $n = 2^{16}$, $\underline{H} = [0.2, 0.4, 0.6, 0.8]$ and an invertible mixing matrix W. For each realization, the same sequence of operations is applied. First, $\underline{X}$ are synthesized using the toolbox described in [30, 31] and relying on a multivariate Circulant Embedded Matrix procedure. As a benchmark, for each component of $\underline{X}$, $S_{X_p}(j)$ is computed as in Eq. 4 and $\hat{H}_{X_p}$ is estimated using Eq. 5. Second, $\underline{Y} = W\underline{X}$ is computed. For each component of $\underline{Y}$, $S_{Y_p}(j)$ and $\hat{H}_{Y_p}$ are estimated. Third, the demixing procedure, proposed in Section 2.2, is applied to $\underline{Y}$ and yields a demixing matrix $\widehat{W^{-1}}$ and demixed time series $\underline{Z} = \widehat{W^{-1}}\underline{Y}$. For each component of $\underline{Z}$, $S_{Z_p}(j)$ and $\hat{H}_{Z_p}$ are estimated. Simulations were repeated for several matrices W. Results are reported for one arbitrarily chosen W as performance were all comparable and conclusions identical.

The results consist of comparing the statistics $\log_2\langle S_{X_p}(j)\rangle_R$, $\log_2\langle S_{Y_p}(j)\rangle_R$ and $\log_2\langle S_{Z_p}(j)\rangle_R$ for each of the $P = 4$ respective components, where $\langle\cdot\rangle_R$ denotes the average over the R realizations (Fig. 1) ; and distributions (by means of boxplots) of $\hat{H}_{X_p} - H_p$, $\hat{H}_{Y_p} - H_p$ $\hat{H}_{Z_p} - H_p$ (Fig. 2).

As expected, for $\underline{X}$, the linear behavior in j of all components of $\log_2\langle S_{X_p}(j)\rangle_R$ is conspicuous, yielding unbiased estimates of H_{X_p}. After mixing, though, all components of $\log_2\langle S_{Y_p}(j)\rangle_R$ display patent departures from linearity. Because the wavelet transform is itself linear and all components of $\underline{X}$ are independent, then $S_{Y_p}(j) = \sum_{p'=1}^{P} \alpha_{p,p'} 2^{j(2H_{p'}-1)}$ for each component of $\underline{Y}$, where the matrix $\alpha = (\alpha_{p,p'})$ depends jointly on $W\Sigma W^T$ and $\underline{H}$. These mixtures of power laws clearly explain the departure from linear behavior for $\log_2\langle S_{Y_p}(j)\rangle_R$ as well as the strongly biased estimates of H_{Y_p}. After demixing, all components of $\log_2\langle S_{Z_p}(j)\rangle_R$ exhibit saliently linear behavior, remarkably superimposing on that of $\log_2\langle S_{X_p}(j)\rangle_R$. This provides a striking illustration of the successful demixing of Y for each realization. In addition, the distributions for $\hat{H}_{Z_p} - H_p$ resemble those of $\hat{H}_{X_p} - H_p$, thus indicating that estimation performance for $\underline{H}$ based on the demixed process Z is comparable to that obtained from the original, premixed X, a very remarkable result.

Further, Fig. 3 shows the estimator distributions (via boxplots) for each of the $P \times P$ entries of $\widehat{W^{-1}} - W^{-1}$. All entries of W^{-1} are remarkably estimated, notably with negligible biases.

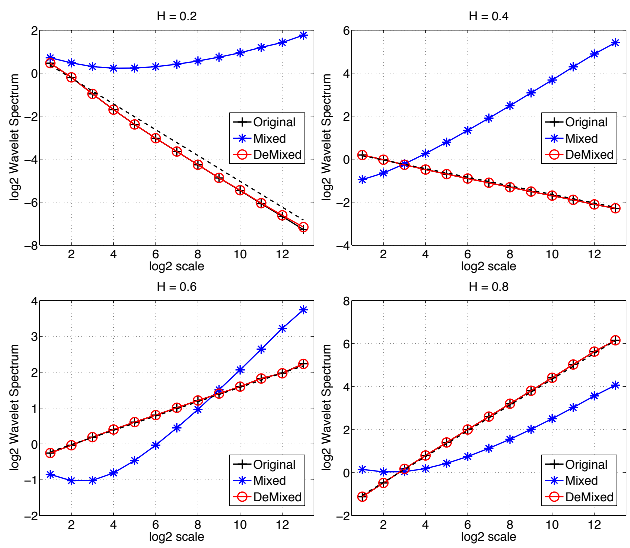

Fig. 1. $\log S(j)$ **vs.** j superimposed for processes $\underline{X}$ (original, black '+'), $\underline{Y}$ (mixed, blue '$*$ ') and $\underline{Z}$ (demixed, red 'o'), for each of the $P = 4$ components, sorted by ascending order of H_p. Dashed black line shows the theoretical power law.

Results not shown due to space constraints further indicate that the proposed procedure remains extremely efficient even for small sample sizes (down to $n = 2^8$), though a precise quantification of the effect of sample size (beyond the scope of the present contribution) actually depends jointly on the choices of $\underline{H}$ and W. Finally, when one is interested in identifying $\underline{H}$ only, the assumption of pairwise distinct H_p can be relaxed. In this case, W is identified up to a multiplication by a rotation matrix that affects only the subspace spanned by the components that share one same H, while the vector $\underline{H}$ itself is well-identified.

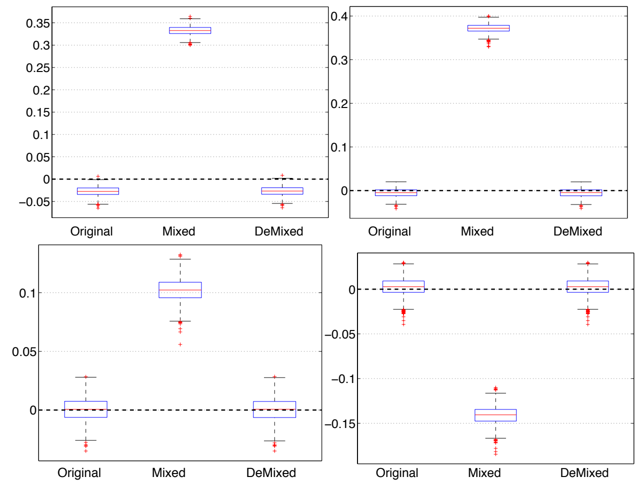

Fig. 2. **Boxplots** $\hat{H}_p - H_p$ obtained from $\underline{X}$ (original, left), $\underline{Y}$ (mixed, middle) and $\underline{Z}$ (demixed, right), for each of the $P = 4$ components, sorted by ascending order of H_p.

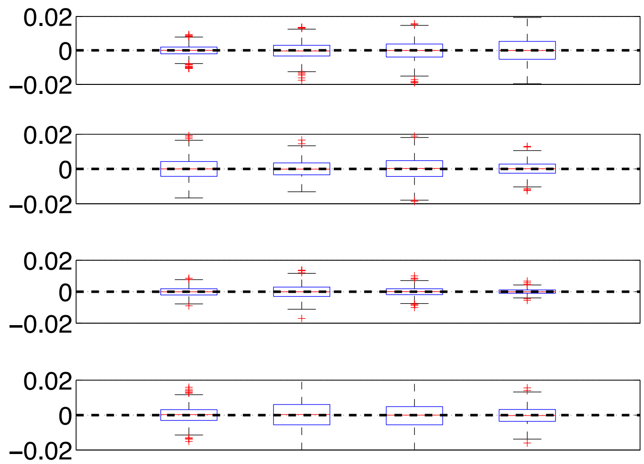

Fig. 3. **Boxplots for the** 4×4 **entries of** $\widehat{W^{-1}} - W^{-1}$.

4. CONCLUSIONS

To the best of our knowledge, the present contribution puts forward the first estimator for the entire set of Hurst parameters $\underline{H}$ for operator self-similarity with non-diagonal mixing matrix W (in the particular case where Σ is diagonal but W is *not*). The proposed procedure also provides a relevant identification of the entire mixing matrix W, which has never been achieved either. Improvements on the current procedure will be further investigated along several lines, such as by comparing exact joint diagonalization of only two estimated covariance matrices against approximate joint diagonalization of several such matrices; or by replacing time domain covariance estimations by wavelet domain ones. Furthermore, we plan to address the general case where Σ is not a priori diagonal. The application of the proposed demixing procedure to multivariate infraslow brain activity data [14] and heart rate variability [12] are currently under investigation.

5. REFERENCES

[1] G. Wornell and A. Oppenheim, "Estimation of fractal signals from noisy measurements using wavelets," *IEEE Transactions on Signal Processing*, vol. 40, no. 3, pp. 611–623, 1992.

[2] E. Masry, "The wavelet transform of stochastic processes with stationary increments and its application to fractional Brownian motion," *IEEE Transactions on Information Theory*, vol. 39, no. 1, pp. 260–264, 1993.

[3] P. Flandrin, "Wavelet analysis and synthesis of fractional Brownian motion," *IEEE Transactions on Information Theory*, vol. 38, pp. 910 – 917, March 1992.

[4] D. Veitch and P. Abry, "A wavelet-based joint estimator of the parameters of long-range dependence," *IEEE Trans. Inform. Theory*, vol. 45, no. 3, pp. 878–897, 1999.

[5] P. Abry, R. Baraniuk, P. Flandrin, R. Riedi, and D. Veitch, "Multiscale nature of network traffic," *IEEE Signal Proc. Mag.*, vol. 19, no. 3, pp. 28–46, 2002.

[6] B. Mandelbrot and J.W. van Ness, "Fractional Brownian motion, fractional noises and applications," *SIAM Reviews*, vol. 10, pp. 422–437, 1968.

[7] P. Flandrin, "Wavelet analysis and synthesis of fractional Brownian motions," *IEEE Trans. Inform. Theory*, vol. 38, pp. 910–917, 1992.

[8] A.H. Tewfik and M. Kim, "Correlation structure of the discrete wavelet coefficients of fractional Brownian motions," *IEEE Trans. Inform. Theory*, vol. IT-38, no. 2, pp. 904–909, 1992.

[9] J.-M. Bardet, G. Lang, G. Oppenheim, A. Philippe, S. Stoev, and M.S. Taqqu, "Semi-parametric estimation of the long-range dependence parameter: A survey," in *Theory and applications of Long-range dependence*, P. Doukhan, G. Oppenheim, and M. S. Taqqu, Eds., Boston, 2003, pp. 557–577, Birkhäuser.

[10] B.B. Mandelbrot, "Intermittent turbulence in self-similar cascades: divergence of high moments and dimension of the carrier," *J. Fluid Mech.*, vol. 62, pp. 331–358, 1974.

[11] E. Foufoula-Georgiou and P. Kumar, Eds., *Wavelets in Geophysics*, Academic Press, San Diego, Calif., 1994.

[12] P.C. Ivanov, L.A. Nunes Amaral, A.L. Goldberger, S. Havlin, M.G. Rosenblum, Z.R. Struzik, and H.E. Stanley, "Multifractality in human heartbeat dynamics," *Nature*, vol. 399, pp. 461–465, 1999.

[13] B. J. He, J. Zempel, A. Snyder, and M. Raichle, "The temporal structures and functional significance of scale-free brain activity," *Neuron*, vol. 66, pp. 353–69, 2010.

[14] P. Ciuciu, P. Abry, and B. J. He, "Interplay between functional connectivity and scale-free dynamics in intrinsic fMRI networks," *NeuroImage*, vol. 95, no. 186, pp. 248–263, 2014.

[15] B. Audit, A. Baker, C.-L. Chen, A. Rappailles, G. Guilbaud, H. Julienne, A. Goldar, Y. d'Aubenton Carafa, O. Hyrien, Cl. Thermes, and A. Arneodo, "Multiscale analysis of genome-wide replication timing profiles using a wavelet-based signal-processing algorithm.," *Nat. Protoc.*, vol. 8, no. 1, pp. 98–110, Dec 2013.

[16] M.S. Taqqu, W. Willinger, and R. Sherman, "Proof of a fundamental result in self-similar traffic modeling," *SIGCOMM Comput. Commun. Rev.*, vol. 27, no. 2, pp. 5–23, 1997.

[17] L. Calvet and A. Fisher, *Multifractal volatility: Theory, forecasting and pricing*, Academic Press, San Diego, CA, 2008.

[18] P. Frankhauser, "L'approche fractale : un nouvel outil dans l'analyse spatiale des agglomerations urbaines," *Population*, vol. 4, pp. 1005–1040, 1997.

[19] G. Didier and V. Pipiras, "Integral representations and properties of operator fractional Brownian motions," *Bernoulli*, vol. 17, no. 1, pp. 1–33, 2011.

[20] G. Didier and V. Pipiras, "Exponents, symmetry groups and classification of operator fractional Brownian motions," *Journal of Theoretical Probability*, vol. 25, no. 2, pp. 353–395, 2012.

[21] P.-O. Amblard and J.-F. Coeurjolly, "Identification of the multivariate fractional Brownian motion," *IEEE Transactions on Signal Processing*, vol. 59, no. 11, pp. 5152–5168, 2011.

[22] P.-O. Amblard, J.-F. Coeurjolly, F. Lavancier, and A. Philippe, "Basic properties of the multivariate fractional Brownian motion," *Bulletin de la Société Mathématique de France, Séminaires et Congrés*, vol. 28, pp. 65–87, 2012.

[23] J. F. Coeurjolly, P.-O. Amblard, and S. Achard, "On multivariate fractional Brownian motion and multivariate fractional Gaussian noise," in *Proceedings of EUSIPCO*, 2010, pp. 557–577.

[24] H. Wendt, A. Scherrer, P. Abry, and S. Achard, "Testing fractal connectivity in multivariate long memory processes," in *IEEE International Conference on Acoustics, Speech and Signal Processing, Taipei, Taiwan, April 19-24*, 2009, pp. 2913–2916.

[25] S. Achard, D.S. Bassett, A. Meyer-Lindenberg, and E. Bullmore, "Fractal connectivity of long-memory networks," *Phys. Rev. E*, vol. 77, no. 3, pp. 036104, 2008.

[26] B. J. He, "Scale-free brain activity: past, present, and future," *Trends in Cognitive Science*, vol. 18, no. 9, pp. 480–487, 2014.

[27] P. Comon and C. Jutten, *Handbook of blind source separation: independent component analysis and applications*, Academic Press, 2010.

[28] R. A. Horn and C. A. Johnson, *Matrix Analysis*, Cambridge University Press, 1985.

[29] S. Mallat, *A Wavelet Tour of Signal Processing*, Academic Press, San Diego, CA, 1998.

[30] H. Helgason, V. Pipiras, and P. Abry, "Synthesis of multivariate stationary series with prescribed marginal distributions and covariance using circulant embedding," *Signal Processing*, vol. 91, no. 8, pp. 1741–1758, 2011.

[31] H. Helgason, V. Pipiras, and P. Abry, "Fast and exact synthesis of stationary multivariate Gaussian time series using circulant embedding," *Signal Processing*, vol. 91, no. 5, 2011.